STUDY OF SLIP AND DEFORMATION IN HIGH PURITY SINGLE CRYSTAL NB FOR ACCELERATOR CAVITIES*

D. Kang, D.C. Baars, A. Mapar, T.R. Bieler#, F. Pourboghrat, MSU, East Lansing, MI 48824, USA
C. Compton, FRIB, East Lansing, MI 48824, USA

Abstract

High purity Nb has been used to fabricate accelerator cavities over the past couple decades, and there is a growing interest in using large grain ingot Nb as an alternative to the fine grain sheets. Plastic deformation governed by slip is complicated in body-centered cubic metals like Nb. Besides the crystal orientation with respect to the applied stress (Schmid effect), slip is also affected by other factors including temperature, strain rate, strain history, and non-Schmid effects such as non-glide shear stresses and twinning/anti-twinning asymmetry. A clear understanding of slip is an essential step towards modeling the deep drawing of ingot slices, and hence predicting the final microstructure/performance of cavities. Two groups of single crystals, with and without a prior heat treatment, were deformed to about 40% engineering strain in uniaxial tension. Differences in flow stresses and active slip systems between the two groups were observed, likely due to the removal of pre-existing dislocations. Crystal plasticity modeling of the stress-strain behavior suggests that the non-Schmid effect is small in Nb, and that the deep drawing process might be approximated with a Schmid model.

INTRODUCTION

Large grain Nb is being investigated for fabricating superconducting radiofrequency (SRF) cavities for particle accelerators, as a promising alternative to the traditional approach using fine grain Nb sheets [1-4]. In the cavity forming process, grain orientations, active slip systems, dislocation substructure, and recrystallization during heat treatments are interrelated from the metallurgical point of view [4] – slip behavior depends on how grains are oriented with respect to the applied stress; slip and interactions of slip systems result in a certain dislocation substructure; the dislocation substructure determines whether recovery or recrystallization occurs, and resulting dislocation substructure may be defective regions that trap magnetic flux [5]. Establishing the correct model for slip systems is particularly important for predicting the microstructural evolution during deep drawing.

For body-centered cubic (bcc) metals, the close packed (hence slip) directions are one of the four <111> directions, and there are no close packed planes like there are in face-centered cubic metals [6]. Planes containing the close packed direction in a decreasing order of inter-planar spacing are {110}, {112}, and {123}. As no stable stacking faults have been found in bcc metals, no slip planes are defined by dislocation dissociations. These features complicate slip in bcc metals.

In bcc metals, edge dislocations have lower lattice friction and are more mobile than screw dislocations at room temperature, and the movement of screw dislocations is the rate controlling factor during plastic deformation [4]. Since screw dislocation motion is thermally activated, it will likely occur by nucleation of kink pairs on well-defined atomic planes. The kink pair nucleation mechanism gives rise to the temperature and strain rate dependence of the flow stress in bcc metals [6].

The low mobility of bcc screw dislocations can be partly explained by the core relaxation theory [7, 8]. The core of a <111> bcc screw dislocation tends to spread onto three symmetric {110} or {112} planes, which results in a non-planar core and lowers the mobility of screw dislocations. Consequently, screw dislocations are affected by non-glide (out of slip plane) shear stresses, which violates the Schmid law. This relaxation also adds to the waviness of slip traces, since cross slip can occur on two of the three {110} or {112} planes to follow a slip plane with a high resolved shear stress. As a result, long, drawn-out screw dislocations are left behind during plastic deformation and are observable.

There has been no consensus thus far regarding the core structure of screw dislocations in Nb [6]. Seeger has argued that the core relaxation depends on both temperature and purity [9, 10]. The fundamental slip planes change from {110} at low temperatures (<100 K) to {112} at higher temperatures due to a change in the core structure. Experimental results from many bcc metals support this theory, though there are exceptions [11-15]. On the other hand, interstitial impurities such as hydrogen stabilize the {110} relaxation [8, 16]. SRF cavities are fabricated from high purity Nb at room temperature, so {112} relaxation should be favored over {110}. However, the forming process could easily lead to hydrogen contamination, so both relaxations may coexist [7].

Another phenomenon unique to bcc metals is the twinning/anti-twinning asymmetry, in which a smaller resolved shear stress is required to move a screw dislocation in the twinning sense of slip than in the anti-twinning sense [7, 17]. The non-planar screw dislocation cores and the twinning/anti-twinning asymmetry give rise to the non-Schmid effects in bcc metals, and affect the critical resolved shear stress for a given slip system to varying extents [7].

The relationship between slip systems changes with deformation due to rotation of the crystal with respect to

*Work supported by the U.S. Department of Energy, Office of High Energy Physics, through Grant No. DE-FG02-09ER41638.
#bieler@egr.msu.edu

ISBN 978-3-95450-178-6

the applied stress [7]. A general rule regarding work hardening is that if operating slip systems have a common slip direction, little hardening results, but if operating slip systems have different slip directions, significant work hardening occurs.

MATERIALS AND METHODS

This work is a continuation of [18] presented at SRF 2013, and the reader is referred to [18] for details regarding sample preparation as well as the characterization methods used. Briefly, samples were extracted from a Ningxia ingot slice with RRR>300 using electro-discharge machining after analyses identified orientations that would favor different combinations of slip systems. The as-received samples were deformed monotonically to 40% engineering strain, and the annealed samples (800 °C/2hr) with nominally the same orientations were deformed *in-situ* in an scanning electron microscope, to enable observations of lattice orientation changes using electron backscatter pattern mapping and slip features on previously polished surfaces.

RESULTS AND DISCUSSION

Figure 1 shows the engineering stress-strain curves of the as-received and annealed samples side by side. The inverse pole figure triangle provides orientations of the tensile axes with respect to sample orientations, overlaid with Schmid factor contours and boundaries without taking into account the non-Schmid effects.

Flow stresses and yield strengths are consistently lower after the 800 °C/2h heat treatment, presumably due to the removal of pre-existing dislocations that were barriers for plastic deformation. Also, there is no longer a slight drop in the flow stress between yield and about 15% strain, which is most significant in sample T. This emphasizes the effect of a lower dislocation content due to annealing.

Samples oriented close to the symmetric boundaries with equal Schmid factors (U, P, and V) are more prone to work hardening due to the interaction of intersecting slip systems, while orientations with the tensile axis away from these boundaries have a low initial hardening rate. Due to the limited number of samples available, several locations are still missing on the triangle and future tests with new orientations will add to the collection.

The non-Schmid effects will displace the symmetric boundaries in the fundamental triangle and the relationship between slip systems (hence the hardening behavior) will change accordingly. However, crystal plasticity modeling of the 9 orientations suggests that the non-Schmid effects are small in Nb, and surprisingly, for most of the samples the Schmid model predicts the stress-strain behavior better than a preliminary examination of the non-Schmid model. Figure 2 shows several examples that compare the experimental and modeling results on the annealed samples, indicating that the Dynamic Hardening model and the Differential-Exponential models are able to capture the broad effects of work hardening but not the evolutionary details, as discussed in more detail in [19], none of which use the non-Schmid approach. This suggests that these simpler Schmid based models may be adequate for simulating deep drawing of large grain Nb.

By correlating the differences between primary and secondary slip systems with the initial hardening behavior, it was argued in [7] that {112} slip accounts for the initial deformation of the as-received samples. To assess the effects of dislocation removal, a similar analysis was performed on the annealed samples, as shown in Fig. 3. Here, the {110} slip system is best able to account for the initial hardening rates – the smaller the difference between primary and secondary {110} slip systems (so that they are more likely to interact with each other), the more hardening a sample tends to have. This

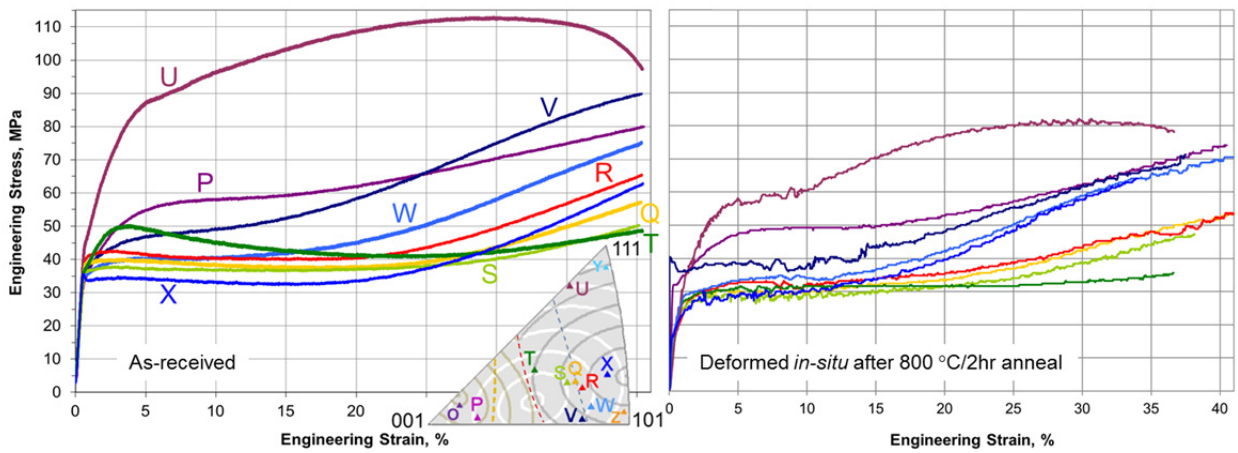

Figure 1: Comparison of stress-strain behavior between as-received (left) and annealed (right) samples. Orientations of tensile axes are indicated by corresponding colors in the triangle inset, which also provides Schmid factor contours in white for {110} slip and gray for {112} slip, both scaled at 0.5, 0.499, 0.49, 0.47, 0.44, 0.40, 0.36, 0.32. Dashed lines mark boundaries with equal Schmid factors (blue – {110}+{112} with the same slip directions, red – {112} with intersecting slip directions, orange – {110}+{112} with intersecting slip directions).

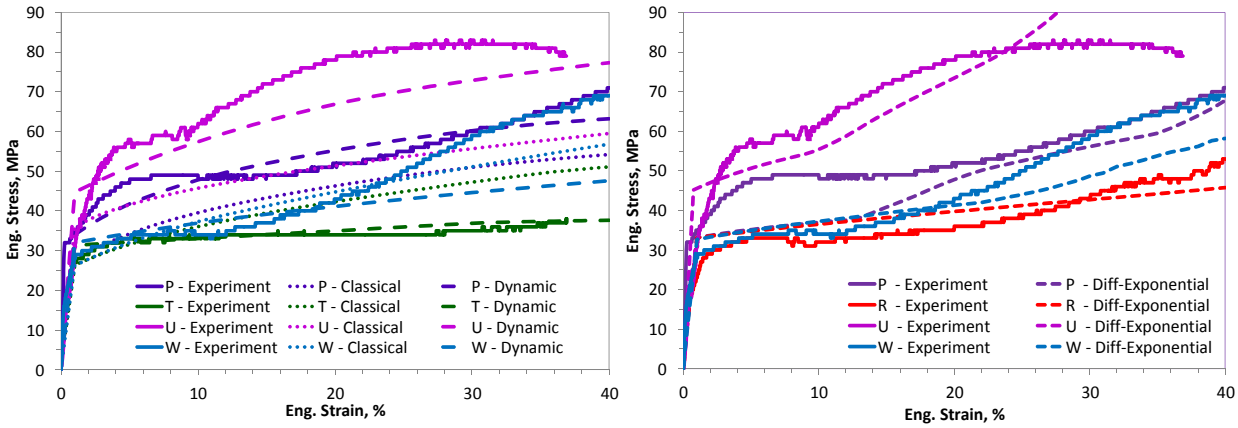

Figure 2: Comparison between the experimental and modeling results of several annealed samples using three modeling approaches [19].

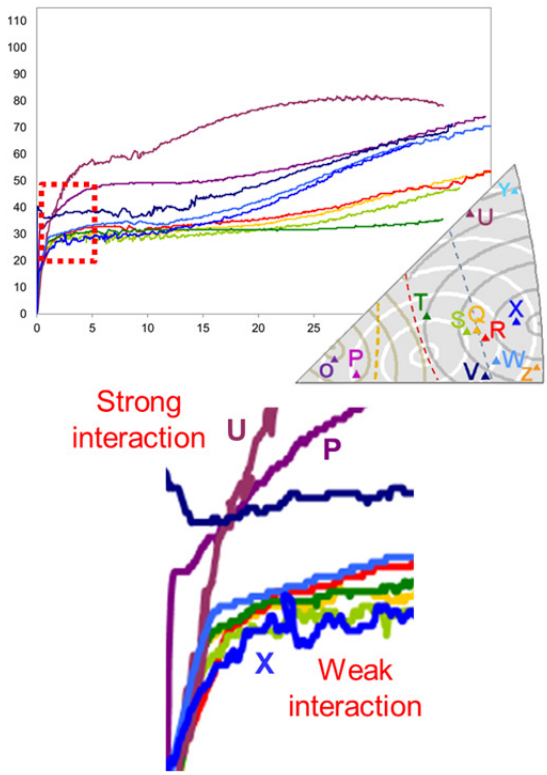

Sample	Ratio of Schmid factors on primary and secondary {110} slip systems	Rank of initial hardening rate
P	1.009	2
V	1.024	3
W	1.096	4
U	1.105	1
T	1.144	5
S	1.187	8
R	1.193	7
Q	1.201	6
X	1.228	9

Figure 3: The table on the right lists the annealed samples in the order of increasing differences between primary and secondary {110} slip systems, which corresponds roughly to decreasing initial hardening rates as shown in the zoomed image on the bottom left.

change in preferred slip systems suggests that the heat treatment may have altered the core structure of screw dislocations in the samples, possibly due to boiling out hydrogen, or that the presence of forest dislocations makes slip on {112} planes more favorable.

The change in dominant slip systems from {112} to {110} is also supported by slip trace analyses on the two groups. Table 1 summarizes the slip planes associated with observed slip traces for the as-received and annealed samples, and the first slip system whose Schmid factor rank is different (evaluated up to the 8th highest) between the two samples is indicated in parentheses. A slip system is marked by red if it was observed in both samples.

There are 6 {112} and 3 {110} slip planes for the as-received group and 3 {112} and 6 {110} slip planes for the annealed group, when considering only the highest ranking slip system systems that were observed. There are 12 {112} and 9 {110} slip planes for the as-received group and 4 {112} and 11 {110} slip planes for the annealed group, when considering slip systems up to 8th in Schmid factor rank. These observations are consistent with the prior argument that the preferred slip systems shifted from {112} to {110} as a result of annealing.

ISBN 978-3-95450-178-6

Table 1: Summary of Slip Planes from Slip Trace Analyses for the As-received and Annealed Samples

	As-received slip planes (Schmid factor rank)	Heat-treated slip planes (Schmid factor rank)
P (same)	112(2),112(5),112(6) 110(8)	112(2) 110(4)
Q (8^{th})	110(3),110(6),110(8)	110(1),110(3)
R (same)	112(4),112(6) 110(2)	110(2)
S (4^{th})	112(2),112(4)	112(5) 110(1)
T (2^{nd})	110(1)	110(1)
U (2^{nd})	112(1),112(7) 110(3),110(4)	112(1) 110(2),110(4)
V (same)	112(2) 110(3)	110(1)
W (1^{st})	112(1)	110(1)
X (4^{th})	112(1)	112(1) 110(2)

Figure 4 shows the evolution of tensile axis orientations with deformation. The trajectories of rotation are similar for orientation S, whereas for other orientations there are varying degrees of discrepancy between the as-received and the annealed samples (X is an extreme). This is again evidence for a change in slip behavior due to the heat treatment that removed pre-existing dislocations.

For the *in-situ* tensile tests on the annealed samples, orientation information was captured in three locations that spanned about 5 mm along the 18 mm gauge length. This allows for assessment of whether the initial orientation gradient within the samples [20] has an influence on deformation. Sample P is an outlier in this regard, since it is the only one that exhibited dramatically different rotations from the three locations. As shown in Fig. 5, it started off with only a slight difference in orientations across the sample, but as deformation proceeds the left and right part of the crystal rotated in opposite directions, leaving the center orientation almost unchanged even after 40% strain. Optical images taken after the test confirmed this counter sense of rotation, as shown in Fig. 6. The resemblance between the as-received and annealed samples suggests that the as-received sample P rotated in a similar manner. However, the fact that no other sample showed this counter sense of rotation may be due to the relatively short distance over which the orientations were recorded. This was imposed by an instrumental limit and could not be overcome at the time of tests.

A limitation of the slip trace analysis it that it can be complicated by the tendency of screw dislocations to cross slip on either {112} or {110} planes [7]. This leads to the problem of "imitation", where frequent cross slip between two slip planes occurs over a small length scale, such that a slip trace looks straight rather than wavy, and is mistaken for a slip trace of the other slip plane family. While dislocation motion unhindered by impurities tends to occur in bursts that should be visible at the scale at which the samples were imaged [7, 21-23], it is unclear if the possibility of imitation can be eliminated.

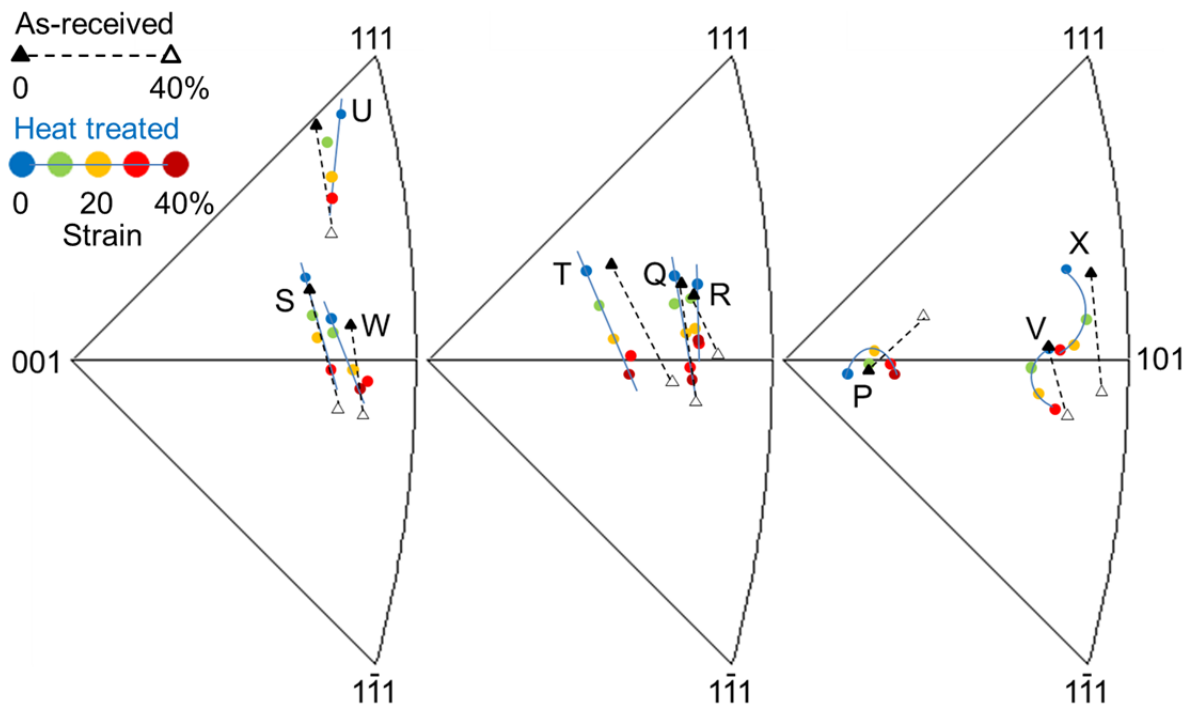

Figure 4: Inverse pole figures showing the evolution of tensile axis orientations with deformation for as-received (triangles) and annealed samples (solid circles).

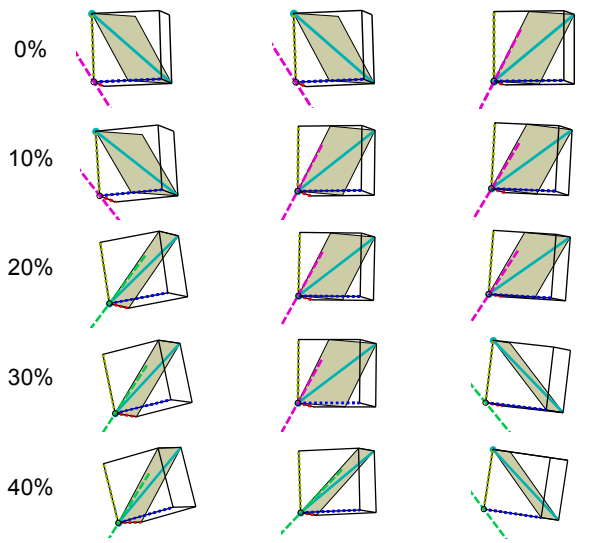

Figure 5: Prisms illustrating how different parts of the annealed sample P rotated in different directions with deformation over a range of about 5 mm along the gauge length.

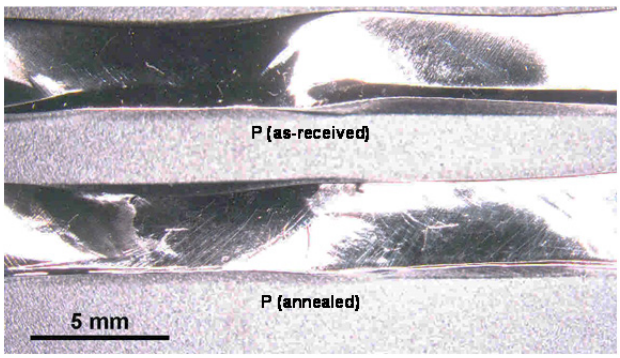

Figure 6: Optical images for the as-received and annealed sample P taken after deformation.

CONCLUSIONS

Nb single crystals with different orientations were deformed before and after annealing, to study slip behavior that will be useful in modeling the deep drawing of large grain ingot slices. Results indicate that the stress-strain behavior is highly dependent on orientations, and that annealing lowered the flow stresses and changed the preferred slip planes from {112} to {110} due to removal of pre-existing dislocations. Initial investigation suggests that a Schmid based model may suffice for simulating the deep drawing process.

REFERENCES

[1] P. Kneisel et al., "Development of large grain/single crystal niobium cavity technology at Jefferson Lab", AIP Conference Proceedings **927**, 84 (2007); doi: 10.1063/1.2770681.

[2] W. Singer et al., "Development of large grain cavities", Physical Review Special Topics - Accelerators and Beams **16**, 012003 (2013).

[3] H. Padamsee, *RF Superconductivity: Science, Technology, and Applications* (2009 WILEY-VCH Verlag GmbH & Co. KGaA, Weinheim).

[4] T.R. Bieler et al., "Physical and mechanical metallurgy of high purity Nb for accelerator cavities", Physical Review Special Topics - Accelerators and Beams **13**, 031002 (2010).

[5] M. Wang et al., "Introduction of precisely controlled microstructural defects into SRF cavity niobium sheet and their impact on local superconducting properties", MOPB018, SRF2015, Whistler, Canada.

[6] C.R. Weinberger et al., "Slip planes in bcc transition metals", International Materials Reviews 2013, Vol. **58**, No. 5.

[7] D. Baars, "Investigation of active slip systems in high purity single crystal niobium", PhD dissertation, Michigan State University 2013.

[8] A. Seeger, U. Holzwarth, "Slip planes and kink properties of screw dislocations in high-purity niobium". Philosophical Magazine, Vol. **86**, Nos. 25-26, pp. 3861, 1-11 September 2006.

[9] A. Seeger, Mater. Sci. Eng. A, 2001, A **319-321**, 254–260.

[10] A. Seeger, J. Phys. IV, 1995, **5**, C7-45–C7-65.

[11] W. Wasserbach, Phys. Stat. Sol. A, 1995, **147**A, 417–446.

[12] W. Wasserbach, V. Novak, Mater. Sci. Eng., 1985, **73**, 197–202.

[13] M.S. Duesbery, et al., J. Phys., 1966, **27**, C3–193–C3–204.

[14] R.A. Foxall, et al., Can. J. Phys., 1967, **45**, 607–629.

[15] R. Maddin, N.K. Chen: J. Met., 1953, **5**, 1131–1136.

[16] A. Seeger, "Progress and problems in the understanding of the dislocation relaxation process in metals", Materials Science and Engineering, A **370**, pp. 50, 2004.

[17] M.S. Duesbery, V. Vitek, "Plastic anisotropy in B.C.C. transition metals", Acta Materialia, Vol. **46** No. 5, pp. 1481, 1998.

[18] D. Kang et al., "Study of slip in high purity single crystal Nb for accelerator cavities", TUP017, Proceedings of SRF2013, Paris, France.

[19] A. Mapar, et al., "Crystal plasticity modeling of single crystal Nb", MOPB057, SRF2015, Whistler, Canada.

[20] D. Kang et al., "Characterizing large grain niobium ingots for accelerator cavities", in preparation.

[21] K.Y. Xie et al., "The effect of pre-existing defects on the strength and deformation behavior of a-Fe nanopillars", Acta Materialia, Vol. **61**, pp. 439, 2013.

[22] N. Friedman et al., "Statistics of dislocation slip avalanches in nanosized single crystals show tuned critical behavior predicted by a simple mean field model", Physical Review Letters, Vol. **109**, pp. 095507, 2012.

[23] S. Papanikolaou et al., "Quasi-periodic events in crystal plasticity and the self-organized avalanche oscillator", Nature, Vol **490**, pp. 517, 2012.

ISBN 978-3-95450-178-6